JOURNAL OF MATERIALS SCIENCE **40** (2005) 1093–1100

Reactive wetting of rutile by liquid aluminium

S. AVRAHAM, W. D. KAPLAN
Department of Materials Engineering, Technion-Israel Institute of Technology, 32000 Haifa, Israel

Sessile drop wetting experiments of liquid Al on polycrystalline rutile (TiO_2) were conducted in the 973–1273 K temperature range under a low total pressure ($\sim 9.3 \times 10^{-3}$ Pa, Ar) and a low oxygen partial pressure ($< 1.33 \times 10^{-7}$ Pa), as a function of temperature and time. A non-wetting ($\sim 150^\circ$, 973 K, $t > 120$ min.) to partial wetting ($\sim 85^\circ$, 1273 K, 50–60 min.) transition reflects reactive wetting characteristics. Microstructural investigations of the metal-ceramic interface shows that TiO_2 is reduced by liquid Al, resulting in the formation of Al_2O_3. The steady-state contact angle at 1273 K of Al on α-Al_2O_3 and Al on rutile are very similar, and the role of Ti segregation is minimal. It appears that spreading of the Al drop on TiO_2 is governed by the reduction reaction at the solid-liquid interface. The measured activation energy corresponds well to the activation energy for volume diffusion of Al, Ti and O in rutile and the volume diffusion of Al in polycrystalline α-Al_2O_3.

1. Introduction

Wetting of ceramics by liquid metals is scientifically and technologically important, and is influenced by a large variety of parameters [1]. The wetting of ceramic phases by liquid metals is a crucial factor during the production of metal-ceramic composites [2, 3]. The wettability of a solid surface is often studied by the measurement of the contact angle, θ, between a liquid drop and the substrate at the three-phase (vapour-liquid-solid) triple junction (see Fig. 1). γ_{sv}, γ_{lv} and γ_{sl} are the surface energies for solid-vapour, liquid-vapour and solid-liquid interfaces, respectively, and are related via Young's equation:

$$\cos(\theta) = \frac{\gamma_{sv} - \gamma_{sl}}{\gamma_{lv}} \quad (1)$$

Wetting can be divided into sub-categories: *non-reactive* and *reactive*. A system is considered non-reactive when mass transfer through the interface is limited and has no (or little) effect on the interfacial energies. Wetting is denoted reactive when a phase is formed as a consequence of interfacial reactions. Two spreading mechanisms are usually considered: diffusion-limited spreading and reaction-limited spreading. In *diffusion-limited spreading* [1], reactions at the triple line are rapid and the supply of reactants to the triple line is the rate limiting factor. Spreading of a drop is regarded as *reaction-limited spreading* [1] when diffusion in the drop is fast, the composition of the drop is constant, and a steady triple line configuration is achieved.

The aim of the present work is to gain basic knowledge about the characteristic wetting behaviour of liquid Al on rutile (TiO_2) in the 973–1273 K temperature range and the nature of the interface reactions that are expected to take place during reduction of TiO_2 by Al.

2. Experimental methods

2.1. Materials

Pure Al was used for the wetting experiments (CERAC, 99.999%). Al cubes ($\sim$50 mg) were polished with a diamond suspension (6 μm surface finish). The resulting sample was cleaned with acetone (technical grade) and ethyl alcohol (95%, practical) in an ultrasonic bath. Chemical etching was conducted by dipping the sample in a NaOH 6.25 M solution for 1 min. The etching process was halted by suspending the sample in distilled H_2O for 30 min.

The polycrystalline TiO_2 (rutile) substrates for wetting experiments were acquired from CERAC Inc. (99.9% purity). The rutile tablets were sliced using a diamond disk blade to a final thickness of $\sim$1.5 mm. The samples were polished using a diamond suspension (0.25 μm surface finish). The resulting substrate was cleaned with acetone (technical grade) and ethyl alcohol (95%, practical). The substrates were heated to 1103 K in a quartz tube furnace in room atmosphere for 30 min. This step was applied in order to clean the substrates from any organic contaminations. X-ray diffraction analysis confirmed that the crystallographic structure of substrate phase was TiO_2 (rutile).

2.2. Wetting experiments

The controlled wetting experiments were conducted in an ultra-high vacuum (UHV) furnace (SURFACE, Germany). The system consists of tungsten heating elements located in a UHV chamber.

The samples were placed on a special storage platform in the UHV chamber (the temperature of the furnace does not affect this section). The UHV chamber was sealed and evacuated to a final pressure of 1.33×10^{-5} Pa. Ar gas (99.999%) was introduced into

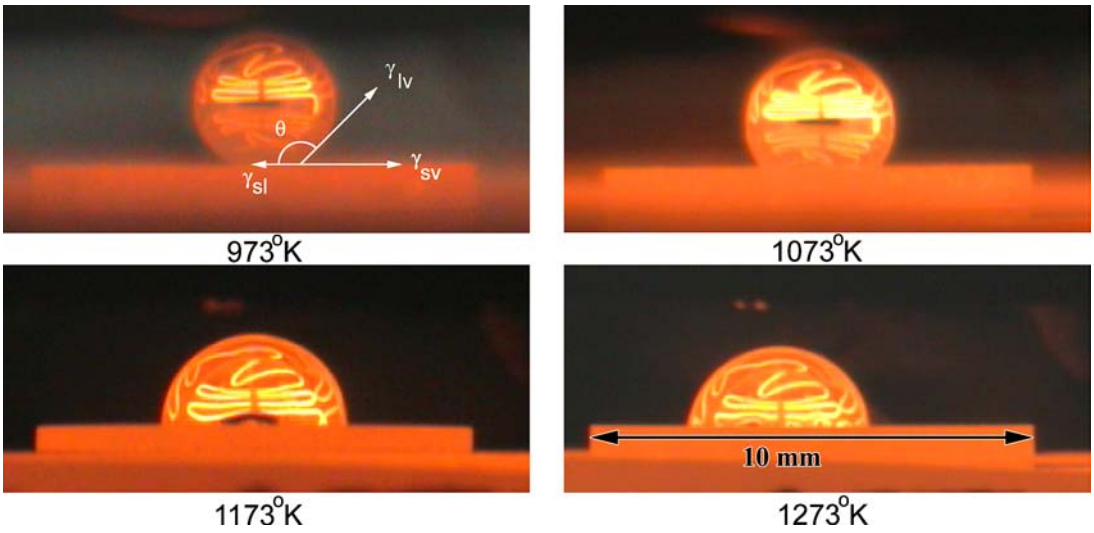

Figure 1 CCD images acquired at the end of the wetting experiments. The pattern on the drop surface is a reflection of the heating elements.

the chamber (0.13 Pa) and the furnace was heated to 1373 K for 60 min. and cooled to room temperature. Surface oxides were sputtered off the solid Al surface prior to wetting using Ar ion sputtering (1.5 kV). This procedure was applied to all six faces of the Al cubes. During the sputtering stage the chamber pressure was kept at 1.33×10^{-3} Pa. After sputtering the Al sample was placed with the substrate on the furnace stage without breaking vacuum. The furnace was heated to the experimental temperature (20 K/min.) while the chamber pressure was kept at 9.3×10^{-3} Pa. The partial pressure of oxygen was monitored ($<1.33 \times 10^{-7}$ Pa) using a micropole residual gas analyzer system equipped with an atomic mass spectrometer. Images of the liquid Al drop were recorded *in-situ* as function of temperature and time via a quartz window. A CCD camera (Avenir, Japan, 150 DPI resolution) was used to record images of the metal drops. Wetting experiments were conducted at 973, 1073, 1173 and 1273 K. The dwell time at each temperature was 2 h. The CCD images were acquired every min during the first five min, and then at five min intervals until the end of the experiment. The contact angle was determined from the images according to geometrical relations [4]. The size of the drops was small, in the order of millimetres, thus the effect of gravity was negligible.

2.3. Characterisation methods

The microstructure of the samples was investigated using atomic force microscopy (AFM) and scanning electron microscopy (SEM). AFM was used to characterize the substrate roughness after polishing. AFM was conducted using an Autoprobe CP (Park Scientific, USA). The microscope was operated in contact mode.

Samples for SEM cross-section were mounted in epoxy resin to limit fracture at the metal-ceramic interface during specimen preparation. The specimens were prepared by diamond disk cutting and diamond polishing of the cross-section (0.25 μm surface finish), followed by carbon coating to prevent charging in the SEM. No etching process was applied. SEM was conducted using a FEI XL-30 microscope, equipped with an energy dispersive spectrometer (EDS) (6506, Oxford Instruments, UK) for microanalysis of the sample (elemental detection limited to $Z > 4$). The accelerating voltage during the analysis was 10 kV and the working distance was 10.5 mm. High resolution SEM was conducted using a LEO 982 Gemini microscope equipped with a Schottky electron source at an accelerating voltage of 3 kV and working distance of 3–5 mm.

3. Results

3.1. Wetting behavior of Al on TiO_2

SEM and AFM analysis of the rutile substrates used for wetting showed that open porosity and surface cracks were evident. The RMS roughness of the sample and average roughness of the substrates were 0.147 μm and 647 Å, respectively.

Fig. 1 presents optical CCD images of the liquid Al drop on the rutile substrate acquired after two hours at the experimental temperatures. Fig. 2 summarizes the contact angle as a function of temperature and time. At 973 K the contact angle seems to be rather constant, stabilizing after 120 min at $\sim 150^\circ$. The contact angles from experiments conducted at 1073 and 1173 K reflect the characteristics of reactive wetting. The contact angle steadily decreases, but no steady-state contact angle value was reached during the experimental period (120 min.). The contact angle at 1273 K presents all the characteristic stages of reactive wetting. The initial contact angle (124°) rapidly decreases, and after 80 min. a steady-state contact angle value is reached ($\sim 86^\circ$).

The change in contact angle as function of time at 973 and 1073 K corresponds to a linear behaviour, but at higher temperatures (1173 and 1273 K) the contact angle decreases exponentially. These features fit well with reactive wetting characteristics [5]. It should be noted that the experimental measurement error in the contact angle evaluation was $\pm 1.5^\circ$.

Fig. 3 presents the change in the drop base radius as a function of the experimental temperature and time. At low temperatures (973 and 1073 K) the triple line velocity is constant with time (9.5×10^{-3} and 27.6×10^{-3} μm/sec, respectively), thus it can

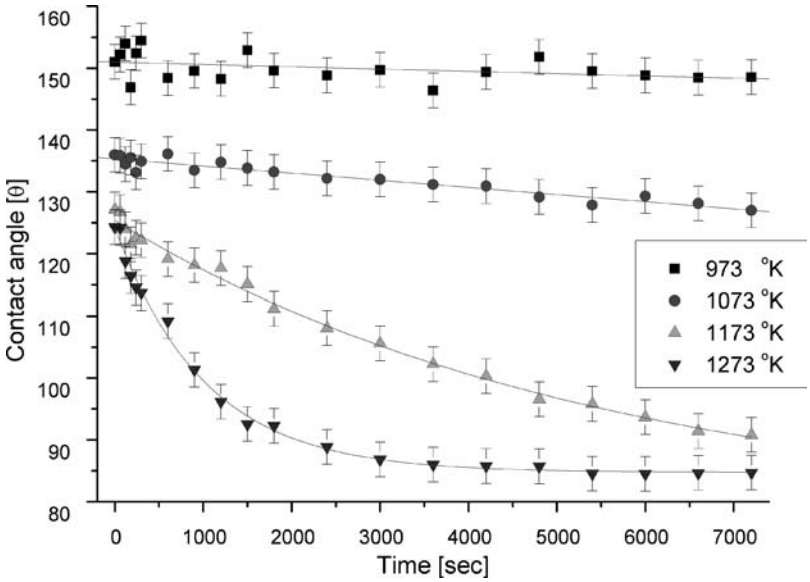

Figure 2 Variation with time of the liquid-solid contact angle.

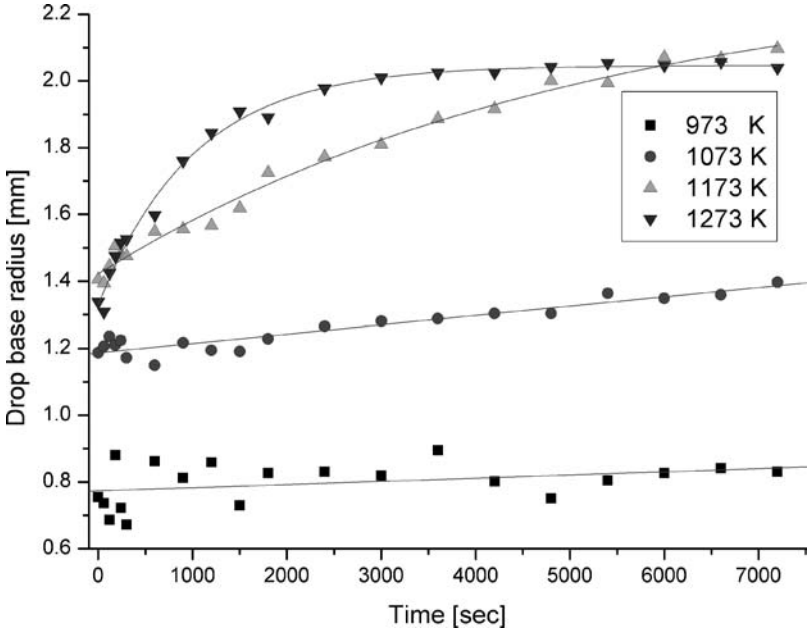

Figure 3 Variation of the drop base radius with time and temperature.

be stated that spreading of the drop at these temperatures is controlled by the rate of the reaction at the liquid-solid interface [6]. At 1173 K the drop base radius variation with time is composed of a short linear stage ($t < 40$ min), followed by a decaying exponential increase of the drop base radius. Analysis of the liquid-solid interface at 1073 and 1173 K showed that the decaying exponential stage is related to the formation of Al_2O_3 at the Al-TiO_2 interface. The spreading rate of the drop reaches 49.08×10^{-3} μm/sec (after 120 min. steady-state is not achieved).

The experimental results acquired at 1273 K present all the characteristics of reactive wetting. The drop base radius variation with time is composed of a brief period ($t < 15$ min) of linear spreading kinetics, followed by a decaying exponential increase of the drop base radius. After 100 min the spreading rate stabilizes at 20×10^{-3} μm/sec.

3.2. Microstructural analysis

Fig. 4a presents a top view, secondary electron (SE) SEM micrograph of the Al drop from the 973 K wetting experiment. An alumina scale which is confined to the top of the drop is visible (confirmed by EDS). The alumina layer occupied only the top of the metallic drop, thus minimizing the effect of the oxide scale on the apparent contact angle. The grooves that are apparent in the micrograph are associated with Al grain boundaries. Fig. 4b presents a top view SE SEM micrograph of the Al drop from the 1273 K wetting experiment. No major oxide scales are visible. The thickness of the natural oxide scale on pure Al formed at temperatures above 573 K is ~300 Å [7]. The total weight change due to evaporation of aluminium or the formation of Al_2O_3 could not be detected, being below 0.001 g. Laurent *et al.* [8] discussed in detail the reduction of Al_2O_3 to gaseous Al_2O by liquid Al at high temperatures and low

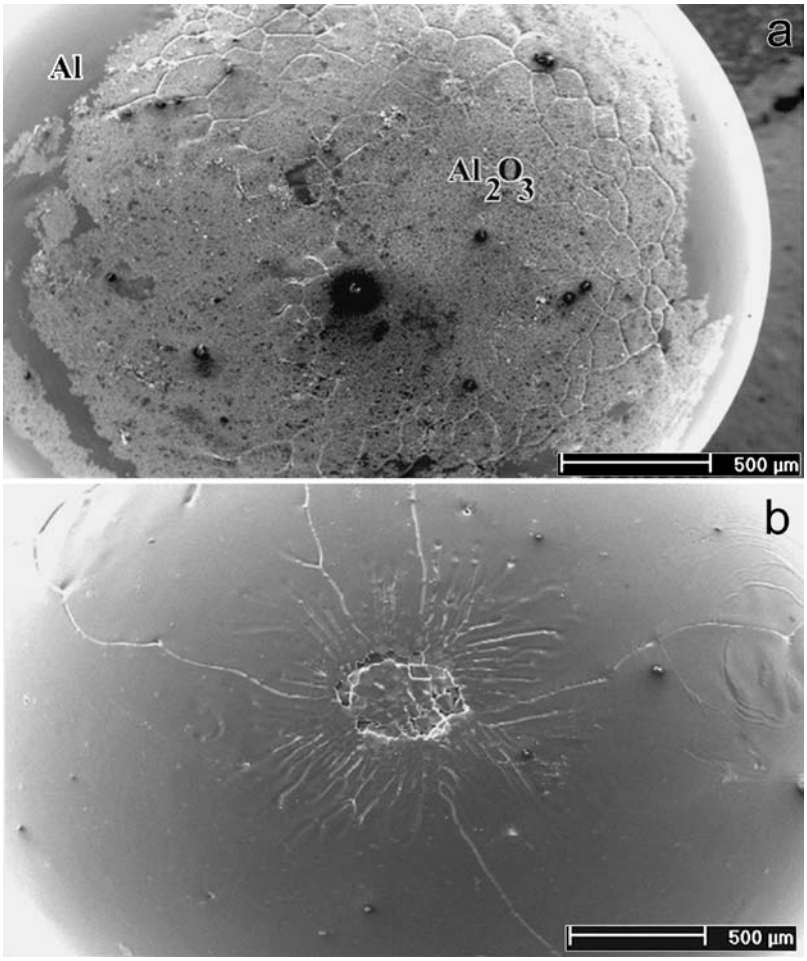

Figure 4 (a) SE SEM micrograph of the Al drop (973 K) and (b) SE SEM micrograph of the Al drop (1273 K).

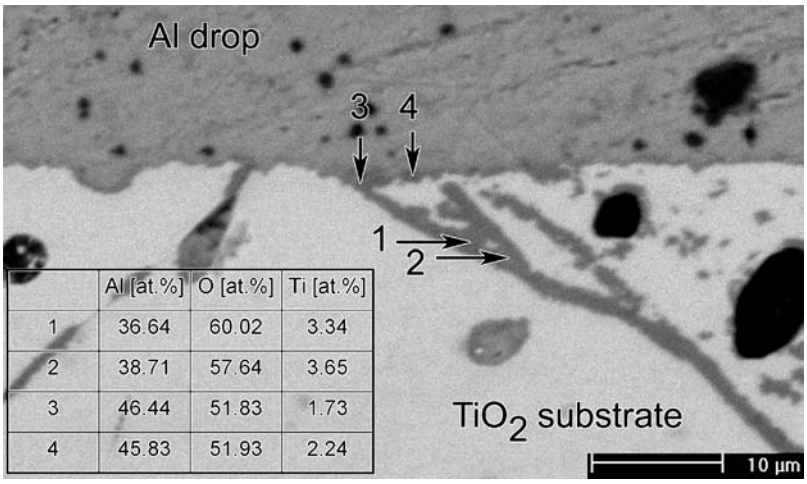

	Al [at.%]	O [at.%]	Ti [at.%]
1	36.64	60.02	3.34
2	38.71	57.64	3.65
3	46.44	51.83	1.73
4	45.83	51.93	2.24

Figure 5 BSE SEM micrograph of the Al drop-substrate interface (1273 K).

oxygen partial pressures, which prevents a continuous oxide scale from forming on the liquid drop.

Fig. 5 presents a cross-section backscattered electron (BSE) SEM micrograph of the Al drop-substrate interface area (1273 K). Points 1–4 indicate the location of quantitative EDS spot analysis. A continuous layer ($\sim$0.5 μm thick) has evolved at the interface, and within cracks in the vicinity of the interface. The composition of the interface layer (with a dark contrast) corresponds to Al_2O_3. The interface measurements (points 3 and 4 in Fig. 5) have an increased Al content and reduced O content compared to stoichiometric Al_2O_3, due to the interaction of the electron beam with the adjacent bulk Al. The measured composition within the cracks (points 1 and 2 in Fig. 5) has a slightly lower Al concentration (and an increased Ti concentration) compared to bulk Al_2O_3, due to the interaction of the electron beam with the adjacent bulk TiO_2. These results are not surprising, since the formation of α-Al_2O_3 is expected as a result of the reduction of TiO_2 by liquid Al [9, 14].

EDS line-scan (interface) analysis of the 973 K wetting couple did not detect an oxygen-rich layer.

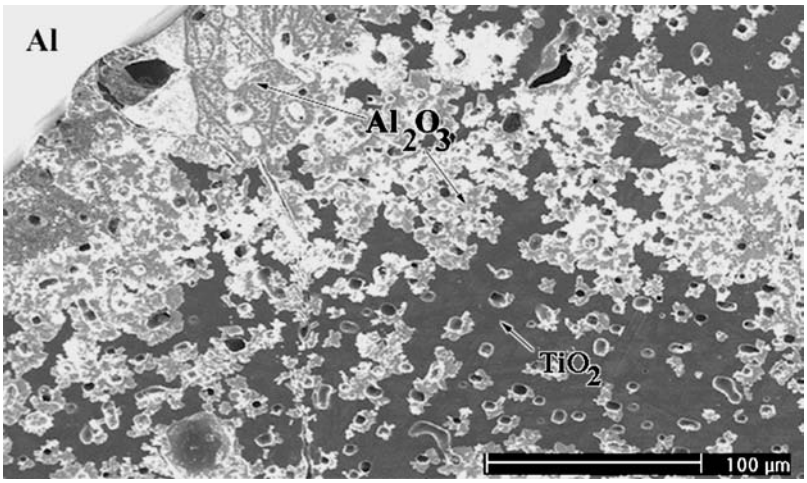

Figure 6 Top view SE micrograph of the Al drop-substrate area (1273 K).

Probably due to thermal expansion coefficient differences, the metal-ceramic interface was cracked. This did not occur for other samples. EDS line-scan measurements of the 1073 and 1173 K wetting couples showed the presence of an oxygen-rich layer. HRSEM analysis showed the presence of an interface layer. The thickness of the interface layer formed at 1073 and 1173 K was 0.16 and 0.3 μm, respectively.

Fig. 6 presents a top view SE-SEM micrograph of the outer perimeter of the Al drop on the substrate surface from the 1273 K experiment. It appears that a thin layer of Al_2O_3 is located at the perimeter of the solidified Al drop. The presence of an Al_2O_3 layer far from the drop perimeter can be attributed to surface diffusion or evaporation-condensation of Al that is followed by the reduction of TiO_2.

4. Discussion

4.1. Interface reaction

TiO_2 is reduced by aluminium according to the following reaction [9]:

$$3TiO_2 + 13Al \rightarrow \cdots \rightarrow 3Al_3Ti + 2\alpha\text{-}Al_2O_3 \quad (2)$$

This reaction is generalized due to the fact that it is divided into sub-reactions that take place in the solid and liquid phase over a wide temperature range. The reduction reaction results in the formation of α-Al_2O_3 and Al_3Ti (based on XRD) [9].

The formation of α-Al_2O_3 results from the reduction of rutile by Al. An expected product is the formation of a titanium-aluminium intermetallic (Al_3Ti). The atomic concentration of titanium in the Al drop was calculated to be $\sim$0.03 at.%, which is based on the thickness of the Al_2O_3 layer measured by HRSEM and Al drop base dimensions measured according to the CCD images (and the density of Al at 1273 K). Analysis of the Al-rich part of the Al-Ti phase diagram [10] shows that the maximum Ti solubility limit in Al at 1273 and 873 K is $\sim$1.5 and 0.1 at.%, respectively.

Thus it is clear that aluminium can easily dissolve 0.03 at.% titanium. Segregation of Ti to the solid-liquid interface should result in a decrease of the contact angle [11], unless this is compensated by segregation to the liquid free surface (and possibly the solid substrate surface). This probably does not occur to a significant amount, based on the similarity between the measured contact angles for Al-TiO_2 and Al-Al_2O_3 at 1273 K [4, 8]. The reduction reaction of TiO_2 by Al results in the formation of Al_2O_3 and the dissolution of Ti atoms in the liquid Al:

$$4Al_{(l)} + 3TiO_{2(s)} \rightarrow 2Al_2O_{3(s)} + 3Ti_{(l)} \quad (3)$$

The contact angle of pure metals (Pt, Au, Ag, Cu and Ni) on Al_2O_3 at high temperatures can be significantly lowered by the addition of small amounts of Ti into the melt [11]. The improved wetting behaviour is attributed to the formation of titanium oxides (TiO and Ti_2O_3) or segregation of titanium at the liquid-solid interface [11], while the exact mechanism is currently a subject of debate [12]. The oxygen that is released during reduction of TiO_2 by liquid Al is consumed by the formation of α-Al_2O_3. The Gibbs energy of formation of α-Al_2O_3 at 1273 K ($\Delta G_{1273^\circ K} = -1270.95$ KJ/mol) [13] is much lower than that of TiO ($\Delta G_{1273^\circ K} = -421.2$ KJ/mol) [13], thus the formation of α-Al_2O_3 is preferred over the formation of TiO.

Sobczak *et al*. [14] measured the final contact angle between Al and titania by a sessile drop method in vacuum after 2 h at 1173, 1273 and 1373 K. The measured contact angles are: 96°, 80° and 64°, respectively. Al_2O_3 was detected as an interface layer at the solid-liquid interface and as precipitates (<20 μm in size) in the vicinity of Al-TiO_2 interfaces and Al-Al_2O_3 interface [14] formed from sessile drop wetting experiments. The formation of the Al_2O_3 precipitates was attributed to dissolution-precipitation mechanism of Al_2O_3 [14]. These kinds of precipitates were not detected in low oxygen partial pressure wetting experiments of Al on Al_2O_3 [4] and in this study. The non-wetting to wetting transition in the Al-Al_2O_3 is motivated by the formation of an oxygen rich layer that lowers the solid-liquid interface energy [4]. The discrepancy between the observations can be attributed to the possible difference in the partial pressure of oxygen, which was not measured by Sobczak *et al*. [14]. Diffusion of oxygen from the system chamber takes place along the solid-liquid

interface [4] and results in the formation of the Al_2O_3 precipitates that were observed by Sobczak *et al*. [14].

4.2. Variation of the contact angle with time

The wetting behaviour of Al on TiO_2 (rutile) that was observed shows the characteristics of reactive wetting. The final (after 120 min.) drop shape is perfectly spherical (see Fig. 1). This is in contrast to the drop shape and advancing contact angle during the initial stages of spreading. The advancing angle is higher than the steady-state angle at 973 K, probably due to the geometrical effect of the substrate surface roughness at the triple line [1].

From wetting experiments at 973 K it was concluded that the contact angle is constant ($\theta \sim 150^\circ$) within the time-frame of the experiment. No reaction product was detected by HRSEM at the liquid-solid interface. The metal-ceramic interface contained cracks, which apparently resulted during cooling of the sample due to the relatively high thermal expansion coefficient of Al compared to that of the TiO_2 substrate (at room temperature $23.5 > 7.4$ [$10^{-6}K^{-1}$]) [15, 16]. The apparent lack of reaction at the interface is strengthened by the difference between the recorded contact angle ($\theta \sim 150^\circ$) and the contact angle between Al and alumina ($\theta \sim 103^\circ$) at 933 K [8]. Thermal analysis by Feng *et al*. [9] showed that a reduction reaction is expected between Al and TiO_2 at 973 K. The lack of apparent reaction products is attributed to the rather short experiment time (2 h) and relatively low temperature (973 K) compared to typical diffusion couple experiments. In addition the contact area (solid-liquid interface of the sessile drop) is relatively small compared to the contact area between the powders used during thermal analysis experiments [9].

At 1073 and 1173 K the characteristics of reactive wetting are apparent. There is a steady decrease of the contact angle, but no constant value was achieved during the experimental period. The measured steady-state contact angle after 2 hours at 1173 K is similar to that measured by Sobczak *et al*. [14]. EDS analysis of the Al-substrate interface area showed evidence for the formation of an Al-Ti oxygen rich layer. The steady decrease of the contact angle is attributed to the formation of Al_2O_3. The apparent contact angle during reactive wetting of heterogeneous surfaces is governed by the surface area fraction of the different phases underneath the liquid drop [17].

An intermediate steady state contact angle value was achieved at 1273 K after 50–80 min. ($\theta = 86^\circ$), when the spreading time is a direct consequence of the slow rate of the reaction. As previously stated, the product of the reaction at the Al-rutile interface was Al_2O_3. Thus the wetting of Al on rutile at 1273 K ($t > 120$ min.) takes place on a thin Al_2O_3 layer ($\sim 0.5\ \mu$m) that was formed by the reduction of rutile. Sessile drop measurements of the contact angle of liquid Al on α-Al_2O_3 (sapphire) showed a non-wetting to partial wetting transition (Ar total pressure $\sim 4 \times 10^{-5}$ Pa, $P(O_2) \sim 1 \times 10^{-15}$ Pa) [8]. The contact angle decreased linearly from $106 \pm 6^\circ$ (at 973 K) to $86 \pm 6^\circ$ (at 1273 K). The steady state contact angle of Al on Al_2O_3 (sapphire) stabilized at 85° (1273 K, Ar total pressure 1.33×10^{-5} Pa, $P(O_2) < 1.33 \times 10^{-7}$ Pa) [4]. The measured steady-state contact angle after 2 h at 1273 K is higher ($86^\circ > 80^\circ$) than that observed by Sobczak *et al*. [14]. The difference in contact angle can be attributed to a possible difference in oxygen partial pressures, which can influence the solid-liquid interface energy [4].

The exponential decrease of the contact angle depends on the steady-state contact angle (θ_F) and initial contact (θ_0) angle [5]:

$$\cos\theta_F - \cos\theta = (\cos\theta_F - \cos\theta_0)\exp(-Kt) \quad (4)$$

The constant K depends on the kinetic reaction constant (K_d) and the difference in chemical potential ($\Delta\mu$) for the reduction reaction [5]:

$$K = K_d P \Delta\mu \quad (5)$$

where $K_d = K_d^0 \exp(-\frac{\Delta E}{RT})$, and ΔE is the activation energy for the reduction of TiO_2 (3). The constant P is related to the molar volume of the reaction product (α-Al_2O_3) [5] and the reaction layer thickness at the liquid drop perimeter [5]. The dependence of the difference of chemical potential ($\Delta\mu$) with temperature (6) for the reduction of TiO_2 by Al (3) can be evaluated according to Dezellus *et al*. [5]:

$$\Delta\mu = RT \ln\left(\frac{a_o^{Al}}{a_o^{\alpha-Al_2O_3}}\right) \quad (6)$$

Due to the low solubility of oxygen in liquid Al (10 at. ppm at 1573 K and 0.3 at. ppm at 1273 K) [18], the activity of oxygen in Al a_o^{Al} was set as 0.3 at. ppm for the whole temperature range. The activity of oxygen in α-Al_2O_3, $a_o^{\alpha\text{-}Al_2O_3} = \exp(\frac{\Delta G_f^{\alpha\text{-}Al_2O_3}}{RT})$, was calculated from the Gibbs energy of formation of α-Al_2O_3 in the 973–1273 K temperature range ($\Delta G_f^{\alpha\text{-}Al_2O_3} = 323.5T - 1681600$ [J]) [13].

Fig. 7 presents the logarithmic plot of $\cos(\theta_F)$-$\cos(\theta)$ as a function of time for Al on TiO_2 at the different temperatures. The steady state contact angle was taken as $\theta_F = 85$. The contact angle values that were measured at 1273 K after 60 min were not taken into account due to the fact that the contact angle approaches a steady-state value and thus the reaction at the liquid-solid interface diminishes. From Fig. 7 it can be seen that the linear fit is good, thus validating the use of Equation 4. The slope of the linear fitting represents the constant K.

The activation energy for the reduction of TiO_2 (3) can be estimated by an Arrhenius plot of $\ln(K/\Delta\mu)$ as function of $1/T$ (Fig. 8). The activation energy of the kinetic reaction constant (K_d) is estimated as $\sim 3.43 \times 10^{-19}$ ($JK^{-1}atom^{-1}$), with an apparent error of $\sim 0.25 \times 10^{-19}$ ($JK^{-1}atom^{-1}$). The activation energy for the reduction of anatase (TiO_2 polymorph) by a molten A356 Al alloy was found to be 4.74×10^{-19} ($JK^{-1}atom^{-1}$) [19]. The effective activation energy measured for the inter-diffusion of Al, Ti and O through a rutile layer was found to be 4.90×10^{-19} [$JK^{-1}atom^{-1}$] [20]. The activation energy for volume diffusion of Al in polycrystalline Al_2O_3 is 4×10^{-19}

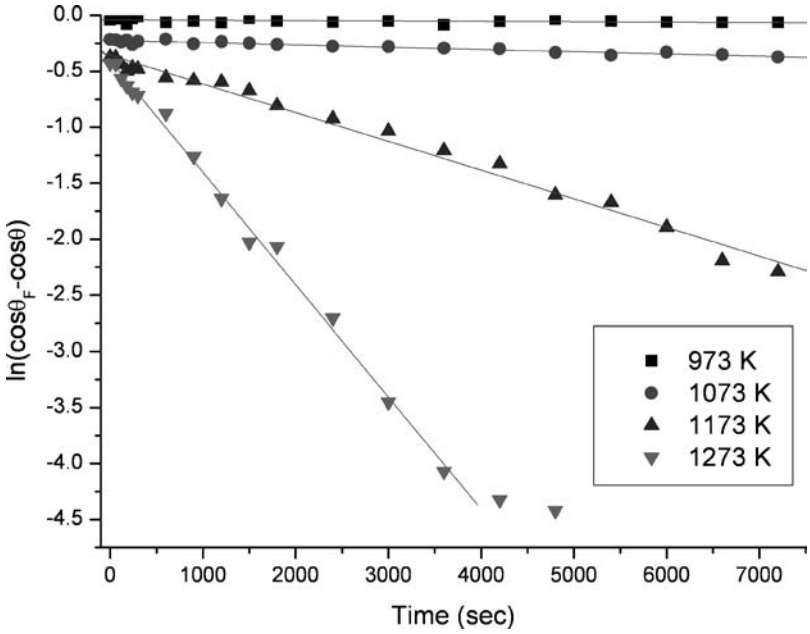

Figure 7 Logarithm of $\cos(\theta_F)$-$\cos(\theta)$ as function of time for Al on TiO_2 at the different temperatures.

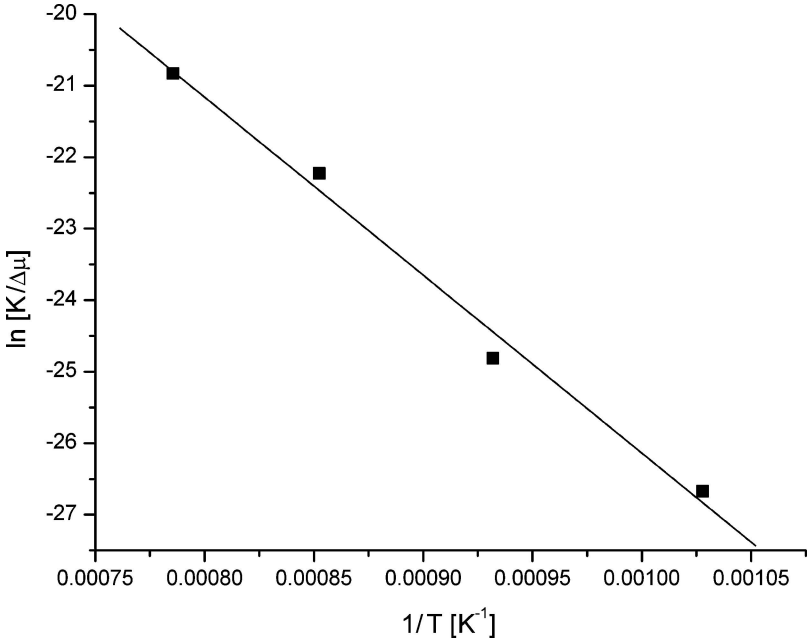

Figure 8 Arrhenius plot of $\ln(K/\Delta\mu)$ as a function of $1/T$.

($JK^{-1}atom^{-1}$) [21]. The similarity of the values with the measured activation energy from Al-TiO_2 wetting experiments suggests that the reduction of TiO_2 by Al is governed by the diffusion of reactive species (Al, Ti, O) through the newly formed Al_2O_3 layer.

Due to the fact that the Gibbs energy of formation of α-Al_2O_3 in the 973–1273 K temperature range does not vary considerably with temperature [13], the change in the chemical potential driving force ($\Delta\mu$) could have been assumed to be constant with temperature. In this case the activation energy of the kinetic reaction constant (K_d) is estimated as $\sim 3.37 \times 10^{-19}$ ($JK^{-1}atom^{-1}$), with an apparent error of $\sim 0.25 \times 10^{-19}$ ($JK^{-1}atom^{-1}$). The two activation energy values are within the experimental error range, thus it can be stated that $\Delta\mu$ is constant in the 973–1273 K temperature range.

5. Summary and conclusions

The characteristic wetting behaviour of liquid Al on rutile in the 973–1273 K temperature range was examined in detail. The interface reaction between Al and rutile results in the reduction of rutile and the formation of Al_2O_3. The Ti content in the Al drop was calculated to be lower than the solubility limit of Ti in solid Al.

At 973 K the contact angle is constant ($\theta \sim 150^\circ$). At higher temperatures reactive wetting was observed. A steady state contact angle value of $\theta = 85^\circ$ was achieved at 1273 K after 120 min. which corresponds to the contact angle between Al and α-Al_2O_3 at 1273 K. The role of Ti segregation at the Al-Al_2O_3 interface seems to be minimal.

Spreading of the Al drop on TiO_2 is governed by the reduction reaction at the solid-liquid interface. The activation energy of the kinetic reaction constant

is estimated as $\sim 3.43 \times 10^{-19}$ ($JK^{-1}atom^{-1}$). The measured activation energy is of the order of magnitude of the effective activation energy measured for the inter-diffusion of Al, Ti and O through a rutile layer and for volume diffusion of Al in polycrystalline Al_2O_3.

Acknowledgements

The authors wish to thank G. Levi, A. Katsman and A. Tvetkov. S.A. was partially supported by a Technion stipend.

References

1. N. EUSTATHOPOULOS, M. G. NICHOLAS and B. DREVET, "Wettability at High Temperatures" (Pergamon, 1999).
2. F. DELANNAY, L. FROYEN and A. DERUYTTERE, *J. Mater. Sci.* **22**(1) (1987) 1.
3. C. GARCIA-CORDOVILLA, E. LOUIS and J. NARCISO, *Acta Mater.* **47**(18) (1999) 4461.
4. G. LEVI and W. D. KAPLAN, *ibid.* **50**(1) (2002) 75.
5. O. DEZELLUS, F. HODAJ and N. EUSTATHOPOULOS, *J. Eur. Ceram. Soc.* **23**(15) (2003) 2797.
6. N. EUSTATHOPOULOS, *Acta Mater.* **46**(7) (1998) 2319.
7. S. WERNICK, R. PINNER and P. G. SHEASBY, "The Surface Treatments and Finishing of Aluminium and Its Alloys," ASM International, 5th ed., (1987). Vol. 1, p. 5.
8. V. LAURENT, D. CHATAIN, C. CHATILLON and N. EUSTATHOPOULOS, *Acta Metall.* **36**(7) (1988) 1797.
9. C. F. FENG and L. FROYEN, *Composites A* **31A**(4) (2000) 385.
10. J. L. MUARRAY (Ed.), "Phase Diagrams of Binary Titanium Alloys," ASM international Metal Park (1987) p. 211.
11. E. SAIZ, R. M. CANNON and A. P. TOMSIA, *Acta Mater.* **48**(18-19) (2000) 4449.
12. L. GREMILLARD, E. SAIZ, J. CHEVALIER and A. P. TOMSIA, *Z. Metallkd.* **95**(4) (2004) 261.
13. IHSAN BARIN, "Thermochemical Data of Pure Substances" (VCH, 1989).
14. N. SOBCZAK, L. STOBIERSKI, W. RADZIWILL, M. KSIAZEK and M. WARMUZEK, *Surf. Interface Anal.* **36** (2004) 1067.
15. E. A. BRANDES AND G. B. BROOK, "Smithells Light Metals Handbook" (Butterworth-Hinemann, 1998) p. 5.
16. M. MIRYAYAMA, K. KOUMOTO AND H. YANAGIDA, "Engineered Materials Handbook" (1991) Vol. 4, p. 748.
17. A. B. D. CASSIE, *Discuss. Faraday Soc.* **3** (1948) 11.
18. S. OTSUKA and Z. KOZUKA, *Trans. Jap. Inst. Met.* **22**(8) (1981) 558.
19. C. W. HSU and C. G. CHAO, *Metall. Mater. Trans. B.* **33B** (2002) 31.
20. R. G. REDDY, X. WEN and I. C. I. OKAFOR, *Metall. Mater. Trans. A.* **32A**(3) (2001) 491.
21. X. B. ZHOU and J. TH. M. DE HOSSON, *J. Mater. Sci.* **30**(14) (1995) 3571.

Received 27 September 2003
and accepted 10 November 2004